The Chlorine Atom Initiated Polymerization of Tetrafluoroethylene

Dana G. Marsh and Julian Heicklen

Contribution from the Aerospace Corporation, El Segundo, California.
Received March 11, 1965

Abstract: Phosgene was photolyzed with 2537-Å. radiation in the presence of tetrafluoroethylene. The phosgene quantitatively decomposes to carbon monoxide and chlorine atoms which are scavenged by the olefin. The resultant radicals can then propagate by addition to the monomer or terminate by combination. No disproportionation products were found. The mechanism is shown in eq. a, b, p, and t. The extent of polymerization was followed at temperatures from 23 to 300° by monitoring the pressure drop during reaction. The carbon monoxide produced acted as an internal actinometer to measure the absorbed radiation. Number-average chain lengths $\bar{n}$ from 2 to 200 were achieved. The ratio $k_p/k_t^{1/2}$ has an activation energy of 5370 ± 300 cal./mole, independent of chain length, but falls measurably as $\bar{n}$ is enhanced. Rotating-sector experiments were performed at 150° and absolute rate constants were computed, assuming no activation energy for termination. Both k_p and k_t rise with $\bar{n}$, the increase in k_t being much more pronounced.

Few studies of the kinetics of gas-phase polymerization of tetrafluoroethylene have been reported in recent years. Arvia, Aymonino, and Schumacher[1] studied the bis(fluorocarbonyl) peroxide induced polymerization over a temperature range of 20 to 40° and at pressures up to 400 mm. They found the reaction to be homogeneous and first order with respect to monomer. The dimerization of gaseous C_2F_4 has been reported by Lacher, Tompkin, and Park,[2] who found the reaction second order and homogeneous. Cordischi, *et al.*,[3] polymerized C_2F_4 by ionizing radiation and found the rate constant with time, dependent on pressure, and independent of intensity of radiation.

We have studied the chlorine atom initiated polymerization of C_2F_4 in the gas phase. The rates were determined over a range of temperatures from 23 to 300°, at various monomer pressures and light intensities.

We studied the polymerization by photodecomposing phosgene using the 2537-Å. resonance line of mercury in the presence of C_2F_4. This technique for producing chlorine atoms has been used previously.[4-6] The sole primary step is the formation of carbon monoxide and chlorine atoms. No side reactions complicate the problem.

Experimental Section

Perfluoroethylene was produced by the decomposition of Teflon. The crude product contained C_2F_4, C_3F_6, cyclo-C_3F_6, n-C_4F_8, and other higher molecular weight components. Pure C_2F_4 was obtained by separation on a Beckman GC-2A gas chromatograph, using a 16-ft. silica gel column. The pure C_2F_4 was analyzed on the gas chromatograph and found to be essentially 100% pure. Matheson high purity phosgene was used; its purity has been determined in previous work.[6] The CO_2 used was also from the Matheson Co. All reactants were degassed twice over liquid nitrogen (−197°) before use.

The reaction mixture was exposed to radiation from a Hanovia, flat, spiral, low-pressure mercury lamp. Mercury was carefully excluded from the vacuum system to prevent sensitized reactions. Pure C_2F_4 was photolyzed, and the lack of product formation confirmed the absence of Hg.

The radiation was filtered through a Corning 9-54 glass filter to remove any radiation below 2200 Å. before reaching the reaction vessel. To change the intensity of the light, Corning 9-30 filters were used. The fraction of light transmitted by these filters was determined on a Cary Model 15 spectrometer. Each filter transmits about 42% of the radiation.

The reaction vessel was surrounded by a furnace, whose temperature was monitored by a thermocouple. Both windows of the cell were covered with a quartz plate to prevent cooling by convection at the window. The temperature of the cell was kept constant to within 2° at all temperatures.

Pressure drops during the polymerization were followed by a Pace Model P7D pressure transducer, in connection with a Type 9804 reluctance gauge input coupler and Type R dynograph recorder manufactured by the Offner Division of Beckman Instruments.

The pressure transducer was calibrated *vs.* a McLeod gauge and is very sensitive to pressure changes, detecting changes of the order of microns. The response is immediate, and no difficulties of response lags were encountered. The rate of pressure drop was obtained from the slopes of the linear portions of the curves during the first 10 to 20% of conversion because deviations from linearity occur at higher conversions.

The absorbed intensity during each run was determined by measuring the CO gas pressure formed during the run.

After the CO was pumped away, the reaction products were separated into fractions over an isopentane slush at −160° and analyzed on the Beckman GC 2A. The gas chromatograph was run isothermally at 130 or 160°. No products were found in either fraction, even for large intensities and low monomer pressures, where the average polymer chain length approached two. By comparison with known standards, it was possible to show that C_4F_8, C_2F_3Cl, C_2F_5Cl, and 1,2-$C_2F_4Cl_2$ were definitely absent.

At higher pressures and lower intensities, higher molecular weight material coated out on the walls and was plainly observable. To prevent this polymer coating from cutting down the absorbed intensity, the face of the reaction vessel was flamed between runs to remove the polymer.

For the experiments at 150°, a rotating-sector disk was inserted between the lamp and the reaction vessel. This disk has five equally spaced openings, each of which allowed total illumination of the cell window. The sector was motor driven, and during each run the speed was measured carefully with a stroboscope.

Results

The initial rates of pressure drop $R(-\Delta P)$ during the photolysis are listed in Table I for various C_2F_4 pressures, absorbed intensities, and temperatures. $R(-\Delta P)$ rises with all three variables. In some runs, excess CO_2 was added but did not alter the results significantly.

(1) A. J. Arvia, P. J. Aymonino, and H. J. Schumacher, *Z. Physik Chem. (Frankfurt)*, **28**, 393 (1961).
(2) J. R. Lacher, G. W. Tompkin, and J. D. Park, *J. Am. Chem. Soc.*, **74**, 1693 (1952).
(3) D. Cordischi, A. Delle Site, M. Lenzi, and A. Mele, *Chim. Ind.* (Milan), **44**, 1101 (1962).
(4) M. H. J. Wijnen, *J. Am. Chem. Soc.*, **83**, 3014 (1961).
(5) M. H. J. Wijnen, *J. Chem. Phys.*, **36**, 1672 (1962).
(6) J. Heicklen, *J. Am. Chem. Soc.*, **87**, 445 (1965).

Table I. Photolysis of C_2F_4-$COCl_2$ Mixtures (λ = 2537 Å.)

$(C_2F_4)/I_a^{1/2}$, (mm. min.)$^{1/2}$	(C_2F_4), mm.	$(COCl_2)$, mm.	I_a, μ/min.	$R(-\Delta P)$, μ/min.	$R(-\Delta P_M)$, μ/min.	$\bar{n}$	$k_p/k_t^{1/2} \times 10^3$ [b]
			Temperature, 23°				
20.9	5.40	25.80	66.7	99.0	166	2.49	23.4
21.1	5.45	24.92	66.7	98.0	165	2.47	22.9
54.6	6.00	25.05	12.0	27.2	39.2	3.27	23.2
54.6	6.00	23.70	12.0	23.8	35.8	2.98	17.9
75.4	19.45	24.21	66.7	171	238	3.56	20.8
75.6	19.52	27.43	66.7	197	263	3.95	25.7
75.6	19.53	22.55	66.7	177	243	3.65	21.8
77.5	20.00	27.20	66.7	198	264	3.97	25.4
77.5	20.00	25.20	66.7	167	234	3.50	19.4
109	5.65	24.65	2.70	8.71	11.4	4.23	20.5
115	6.00	25.00	2.70	8.54	11.2	4.14	18.6
182	20.00	24.80	12.0	45.0	56.7	4.85	15.7
228	59.0	25.00	66.7	540	540	8.10	26.8
247	5.40	24.87	0.478	2.50	2.9	6.07	16.5
385	20.00	25.15	2.7	21.0	21.0	7.94	15.4
385	20.00	25.05	2.7	24.7	24.7	9.15	18.6
543	59.7	25.00	12.0	172	172	14.3	22.6
603	155.6	25.00	66.7	883	883	13.2	18.7
1150	20.00	25.10	0.478	5.13	5.13	10.7	7.6
1160	60.4	25.00	2.7	49.8	49.8	18.4	16.4
1355	149.1	25.00	12.0	199	199	16.6	10.8
1415	155.6	25.00	12.0	232	232	19.4	12.3
2740	59.9	25.00	0.478	9.38	9.38	19.6	6.4
2990	155.7	25.00	2.7	48.6	48.6	18.0	5.3
6770	148.0	25.00	0.478	14.6	14.6	30.5	4.6
			Temperature, 100°				
24.3	6.00	25.00	61.0	243	304	4.98	123
121	6.00	24.20	2.46	39.6	39.6	16.1	117
192	20.00	25.00	10.8	172	172	15.8	72.0
556	57.8	25.00	10.8	264	264	24.3	40.2
957	20.00	25.00	0.437	21.1	21.1	48.3	48.4
957	20.00	25.00	0.437	17.5	17.5	40.0	45.6
1150	57.0	25.00	2.46	70.2	70.2	28.5	23.1
2840[a]	59.4	25.00	0.437	31.1	31.1	71.2	24.3
			Temperature, 150°				
17.4	6.00	25.00	119.64	680.0	680.0	5.70	213.2
34.7	6.00	25.00	29.91	324.0	324.0	10.85	255.2
57.8	20.00	24.70	119.64	1464.0	1464.0	12.24	177.1
57.8	20.00	25.00	119.64	1376.0	1376.0	11.50	164.3
115.6	20.00	25.00	29.91	529.0	529.0	17.69	135.7
172.7	60.00	25.00	120.80	2440.0	2440.0	20.20	105.4
181.3	63.00	25.00	120.80	2440.0	2440.0	20.20	100.5
817.2	63.50	25.00	6.04	236.0	236.0	39.07	45.4
860.3	60.00	25.00	4.86	153.3	153.3	33.33	36.3
3686	57.50	25.00	0.243	42.2	42.2	173.7	46.6
			Temperature, 200°				
21.7	6.00	24.75	76.0	620	620	8.16	284
21.7	6.00	25.00	76.0	625	625	8.22	286
51.6	6.00	26.45	13.5	234	234	17.3	298
72.5	20.00	25.00	76.0	1690	1690	22.2	279
108	6.00	25.05	3.06	90.4	90.4	29.5	254
217	60.0	25.00	76.0	2310	2310	30.4	131
258	6.00	25.05	0.544	43.2	43.2	79.4	300
362	20.00	25.00	3.06	131	131	42.8	113
1060[a]	58.4	25.00	3.06	321	321	105	97
2580	60.0	25.00	0.544	118	118	217	83
			Temperature, 300°				
18.1	6.00	25.00	110	2110	2110	19.2	940
42.9	6.00	24.00	19.6	684	684	34.9	767
90.1	6.00	25.00	4.45	247	247	55.5	594
143	20.00	26.45	19.6	1220	1220	62.2	422
180	59.8	25.00	110	4630	4630	41.9	224
213	6.00	25.40	0.794	64.3	64.3	81.0	371
709	20.00	24.00	0.794	67.6	67.6	84.8	115
709	20.00	25.00	0.794	66.5	66.5	83.8	115
709	20.00	25.10	0.794	106	106	134	184
709[a]	20.00	25.00	0.794	67.6	67.6	84.4	115
709[a]	20.00	25.00	0.794	130	130	164	226
709[a]	20.00	25.00	0.794	91.4	91.4	115	158
2090	59.0	25.00	0.794	156	156	196	93
2090[a]	59.4	25.00	0.794	58.5	58.5	73.7	34.4

[a] 540 ± 50 mm. of CO_2 also present. [b] In (mm. min.)$^{-1/2}$.

The absorbed intensity I_a is simply the rate of CO appearance.[4-6] Experiments were done at several temperatures between 23 and 300° and for C_2F_4 pressures from 5.40 to 155 mm. At any temperature, the fundamental variable of the system is $(C_2F_4)/I_a^{1/2}$, and it was varied by a factor of 325. For the runs at 150°, the high-speed sector experiments are included in Table I, with the average absorbed intensity.

The pressure of phosgene was held constant at about 25 mm. At that pressure, the absorption is less than 50%, and variations in radical concentrations throughout the cell are minimal.[6]

Corning 9-30 filters were used in blocks of two, four, and six to vary the intensity by a factor of 140. The output of the lamp was determined for a number of runs and found to be constant within 8% over a period of 35 days. An average value of I_a was computed for full intensity of the lamp. The I_a values for reduced intensities were then calculated using transmission factors for the 9-30 filters previously determined on a Cary Model 15 spectrometer. These computed I_a values were compared to experimentally obtained values, and the agreement was to within 3%.

Since such good agreement was obtained, the I_a values listed in Table I are calculated values, based upon the absorbed intensity at each temperature with no filters present. The full intensity values are different at the various temperatures since the extinction coefficient is a temperature-dependent function.

Discussion

The reaction sequence that explains the propagation and termination mechanism and is consistent with the data is

$$COCl_2 + h\nu \longrightarrow CO + 2Cl \quad (a)$$

$$C_2F_4 + Cl \longrightarrow C_2F_4Cl \quad (b)$$

$$(C_2F_4)_nCl + C_2F_4 \longrightarrow (C_2F_4)_{n+1}Cl \quad (p)$$

$$(C_2F_4)_nCl + (C_2F_4)_mCl \longrightarrow (C_2F_4)_{n+m}Cl_2 \quad (t)$$

The first two reactions are the initiation steps, whereas (p) represents the propagation and (t) the termination steps. The disproportionation reactions involving transfer of a chlorine or fluorine atom have been omitted because of our failure to find C_4F_8, C_2F_3Cl, C_2F_5Cl, or 1,2-$C_2F_4Cl_2$ as products even for chain lengths approaching two.

Earlier studies[4-6] have shown that the COCl radical is unimportant and that the Cl atom is completely scavenged by the olefin. These results are respectively confirmed in this system by the invariance of the CO production with changing C_2F_4 pressure and the absence of 1,2-$C_2F_4Cl_2$ as a product.

If the polymer is completely deposited, *i.e.*, has a vapor pressure below our detection limits, then the rate of monomer consumption $R(-\Delta P_M)$ equals the rate of pressure drop $R(-\Delta P)$. This situation applies for long chain polymers. On the other hand, for short polymers, the product can remain in the vapor phase and the mechanism would predict that

$$R(-\Delta P_M) = R(-\Delta P) + I_a \quad (1)$$

For experiments in which the quantum yield of pressure drop was small, it was noticed that after sufficient exposure the pressure drop *vs.* time curves had a discontinuity and became steeper. We felt this discontinuity to occur when the vapor pressure of the products was reached. Consequently, for these runs eq. 1 was used to compute $R(-\Delta P_M)$, while for runs with more significant pressure drops, $R(-\Delta P_M)$ was equated with $R(-\Delta P)$. Then, the number-average chain length $\bar{n}$ can be computed from the expression

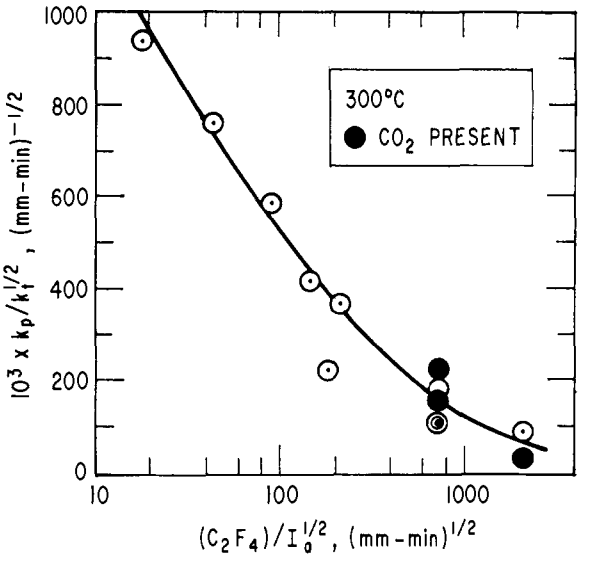

Figure 1. Semilog plot of $k_p/k_t^{1/2}$ *vs.* $(C_2F_4)/I_a^{1/2}$ at 300°.

$$\bar{n} = \frac{R(-\Delta P_M)}{I_a} \quad (2)$$

The values of $R(-\Delta P_M)$, as well as $\bar{n}$, are listed in Table I. The $\bar{n}$ increases with $(C_2F_4)/I_a^{1/2}$, and average chain lengths up to 200 were achieved. For $\bar{n}$ below about 6, the polymer has a sufficient vapor pressure to remain in the gas phase during the initial stages of the experiment; however, for larger $\bar{n}$, the vapor pressure of the polymer is apparently below the sensitivity of the transducer (*i.e.*, 20 μ).

The average values of the propagation constant k_p and the termination constant k_t are defined as

$$k_p = \frac{1}{(R)} \sum_n k_{p(n)}(C_2F_4)_nCl \quad (3)$$

$$k_t = \frac{1}{(R)^2} \sum_{n \leq m} k_{t(n,m)}[(C_2F_4)_nCl][(C_2F_4)_mCl] \quad (4)$$

where (R) is some average radical concentration and $k_{p(n)}$ and $k_{t(n,m)}$ are the specific propagation and termination constants, respectively. The mechanism then leads to the expression

$$\frac{k_p}{k_t^{1/2}} = \frac{I_a^{1/2}(\bar{n} - 2)}{[C_2F_4]} \quad (5)$$

The values of $k_p/k_t^{1/2}$ were computed and are listed in Table I. They are also plotted *vs.* $(C_2F_4)/I_a^{1/2}$ for the 300° runs in Figure 1. At all temperatures, $k_p/k_t^{1/2}$ falls with an enhancement of $(C_2F_4)/I_a^{1/2}$, and thus with an increase of $\bar{n}$. Diffusion to the wall is more important at low pressures and low absorbed intensity. Nevertheless, changing the monomer pressure or the intensity does not alter the results so long as $(C_2F_4)/I_a^{1/2}$ is kept constant. Thus, the likelihood of wall reactions

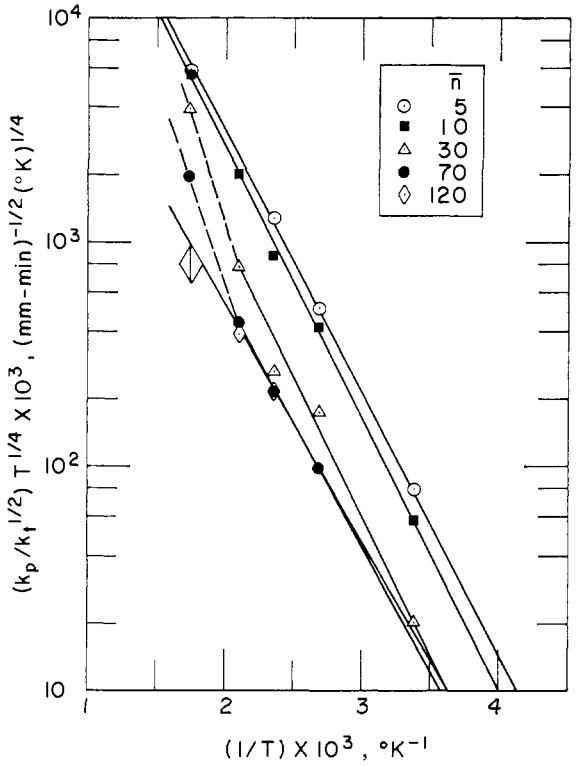

Figure 2. Semilog plot of $(k_p/k_t^{1/2})T^{1/4}$ *vs.* T^{-1} for $\bar{n}$ values 5, 10, 30, 70, and 120.

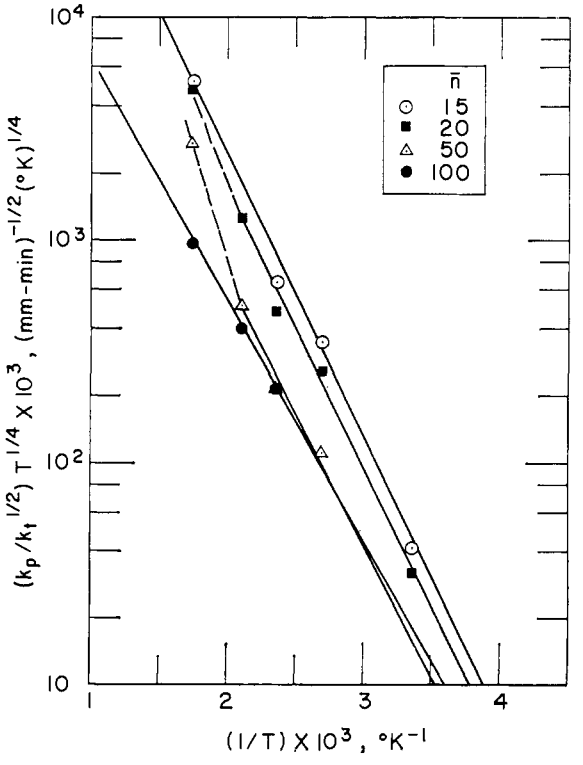

Figure 3. Semilog plot of $(k_p/k_t^{1/2})T^{1/4}$ *vs.* T^{-1} for $\bar{n}$ values 15, 20, 50, and 100.

is small. To further check this point, some runs corresponding to large chain lengths were performed with excess CO_2 added to inhibit diffusion to the walls. Within experimental error, the results were unchanged. Consequently, wall reactions cannot be important in our system.

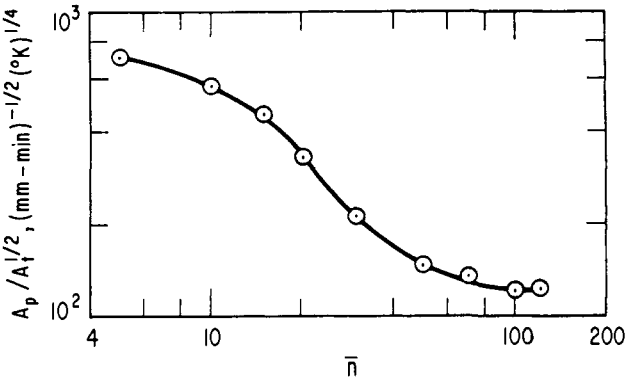

Figure 4. Log-log plot of $A_p/A_t^{1/2}$ *vs.* $\bar{n}$.

In terms of the Arrhenius parameters, the rate constant ratio should be

$$\frac{k_p}{k_t^{1/2}} = \frac{A_p}{A_t^{1/2}} T^{-1/4} \exp\left(-\frac{E_p - E_t/2}{RT}\right) \qquad (6)$$

where A_p and A_t are constants characteristic of the propagation and termination steps, respectively, and E_p and E_t are, respectively, the activation energy for propagation and termination. The temperature dependence in the pre-exponential term corrects for the collision frequency when $k_p/k_t^{1/2}$ is expressed in units of pressure and time.

Working graphs of $\bar{n}$ *vs.* $(C_2F_4)/I_a^{1/2}$ were made; thus, values of $k_p/k_t^{1/2}$ as a function of $\bar{n}$ could be computed. Semilog plots of $(k_p/k_t^{1/2})T^{1/4}$ *vs.* T^{-1} are shown in Figures 2 and 3 for various values of $\bar{n}$. Except at high temperatures where deviations for intermediate values of $\bar{n}$ seem to occur, the plots are linear. The Arrhenius parameters for various $\bar{n}$ are listed in Table II. For $\bar{n}$ from 5 to 120, the activation energy difference is remarkably constant at a value of 5.37 ± 0.30 kcal./mole. Thus, all the dependence of the rate constant ratio with $\bar{n}$ is due to steric effects in accordance with expectation.

Table II. Arrhenius Parameters

$\bar{n}$	$E_p - E_t/2$, kcal./mole	$A_p/A_t^{1/2}$,[a] (mm. min.)$^{-1/2}$ (°K.)$^{1/4}$	$A_p/A_t^{1/2}$,[b] (mm. min.)$^{-1/2}$ (°K.)$^{1/4}$
5	5.32	667 ± 21	712 ± 27
10	5.56	717 ± 31	568 ± 46
15	5.84	832 ± 75	460 ± 47
20	5.72	526 ± 43	331 ± 40
30	5.70	327 ± 28	212 ± 27
50	5.38	151 ± 6	149 ± 6
70	5.06	93 ± 3	136 ± 3
100	4.95	79 ± 3	123 ± 11
120	4.82	69 ± 3	129 ± 11
Average	5.37 ± 0.30		

[a] Using measured $E_p - E_t/2$. [b] Using average $E_p - E_t/2$.

It is not clear why the Arrhenius plots deviate at high temperatures. Perhaps the C–Cl bond in the polymer is broken rapidly, additional polymer is formed, and $k_p/k_t^{1/2}$ appears larger than it should be.

Figure 4 is a log–log plot of $A_p/A_t^{1/2}$ *vs.* $\bar{n}$. The ratio decreases continuously as $\bar{n}$ rises from 5 to 120. The effect is most marked at average chain lengths of about 15 to 40.

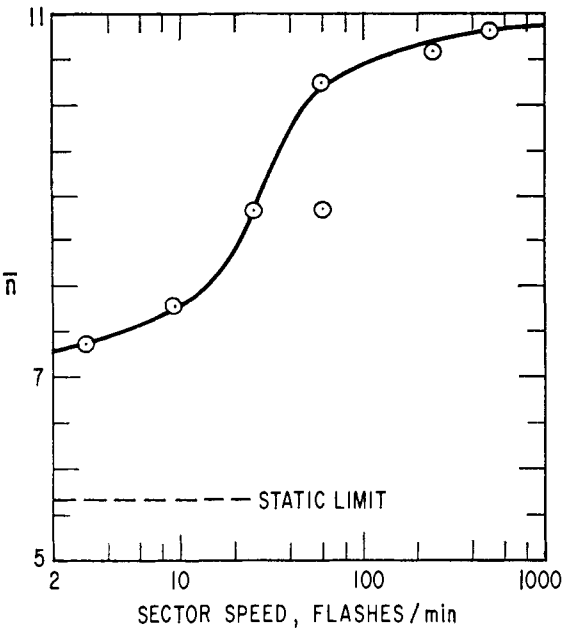

Figure 5. Semilog plot of $\bar{n}$ *vs.* sector speed for (C_2F_4) = 6.0 mm., $(COCl_2)$ = 25.0 mm.; ratio of dark-to-light period is 3.00; average rate of CO production is 29.9 μ/min. (119.6 μ/min. during light period).

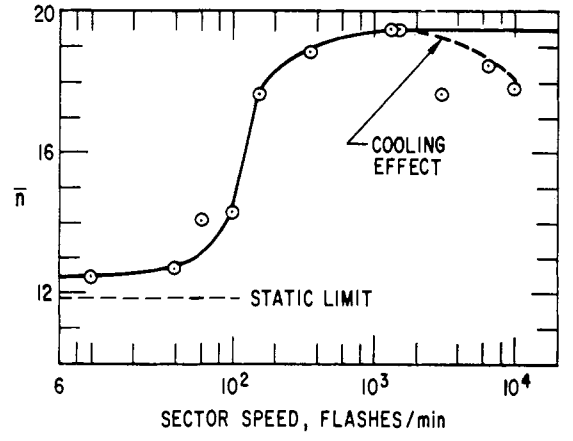

Figure 6. Semilog plot of $\bar{n}$ *vs.* sector speed for (C_2F_4) = 20.0 mm., $(COCl_2)$ = 24.8 mm.; ratio of dark-to-light period is 3.00; average rate of CO production is 29.9 μ/min. (119.6 μ/min. during light period).

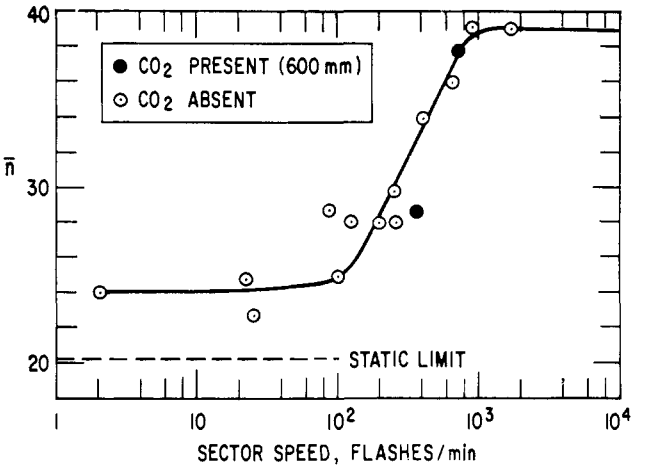

Figure 7. Semilog plot of $\bar{n}$ *vs.* sector speed for $(C_2F_4) \sim 60$ mm., $(COCl_2)$ = 25.0 mm.; ratio of dark-to-light period is 19.0; average rate of CO production is 6.04 μ/min. (120.8 μ/min. during light period).

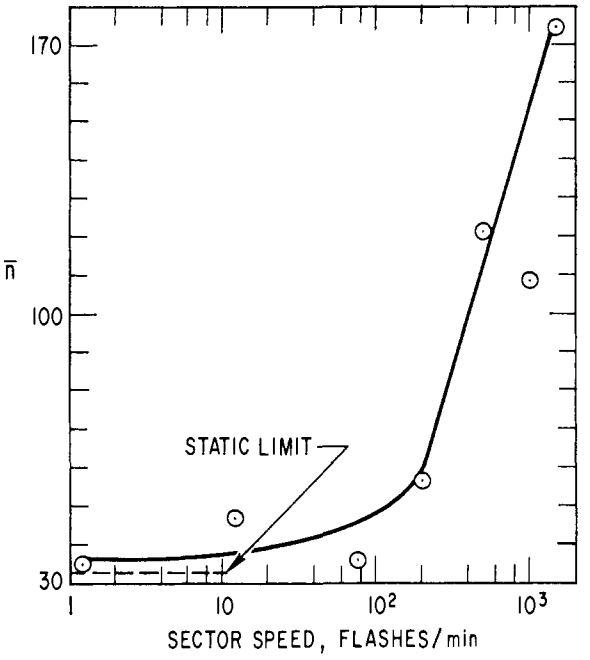

Figure 8. Semilog plot of $\bar{n}$ *vs.* sector speed for $(C_2F_4) \sim 60$ mm., $(COCl_2)$ = 25.0 mm.; ratio of dark-to-light period is 19.0; average rate of CO production is 0.243 μ/min. (4.86 μ/min. during light period).

The results of the sector experiments are shown graphically in Figures 5–8. For these experiments, $R(-\Delta P_M)$ is equal to $R(-\Delta P)$ and $\bar{n}$ was computed from eq. 2. The average chain length is constant at low sector speeds, rises sharply when the sector speed is comparable to the radical lifetime, and finally levels off at large sector speeds. For the runs shown in Figure 6, there is some drop-off in $\bar{n}$ at extremely high speeds. However, at these speeds the sector is acting as a fan and the drop-off can be attributed to cooling.

On the same plots depicting the runs with the rotating sector, the static limit values of $\bar{n}$, obtained without the sector, are shown. In all cases, these values lie below the limiting low-speed sector values. In principle, they should coincide, were the sector openings sufficiently large. However, in any system, the whole reaction cell does not have the same illumination during the transition from the dark-to-light period. As a result, diffusion occurs, and the intermittent space effect enhances n. For our system, with relatively small sector openings, the effect is readily observed.

The theory dealing with effects of rotating sectors on polymerization reactions is well understood. If $k_p/k_t^{1/2}$ is independent of chain length, then $\bar{n} - 2$ at high speeds should be $\sqrt{s}$ that at low speeds, where $s - 1$ is the ratio of dark-to-light periods. In Figures 5, 6, and 8 where $\bar{n}$ is about 10, 15, and 100, respectively, nearly the full effect is observed. As can be seen from Figure 4, $k_p/k_t^{1/2}$ does not vary markedly at these chain lengths. However, for the chain lengths of about 30 corresponding to Figure 7, much less than the full effect is observed, as would be expected if $k_p/k_t^{1/2}$ were falling with increasing $\bar{n}$. Thus, the results of the

Table III. Absolute Value of Rate Constants

$\bar{n}$	k_p at 150°: (mm. min.)$^{-1}$	k_p at 150°: l. (mole sec.)$^{-1}$	A_p: (°K.)$^{1/2}$ (mm. min.)$^{-1}$	A_p: l. [mole sec. (°K.)$^{1/2}$]$^{-1}$	$\pi\sigma_p^2$, Å.^{2}
9	170	0.75×10^5	2.1×10^6	2.2×10^6	0.025
18	260	1.14×10^5	3.3×10^6	3.4×10^6	0.039
30	710	3.1×10^5	8.9×10^6	9.3×10^6	0.106
114	3900	17.2×10^5	49×10^6	51×10^6	0.58

$\bar{n}$	k_t at 150°: (mm. min.)$^{-1}$	k_t at 150°: l. (mole sec.)$^{-1}$	A_t: (°K.)$^{1/2}$ (mm. min.)$^{-1}$	A_t: l. [mole sec. (°K.)$^{1/2}$]$^{-1}$	$\pi\sigma_t^2$, Å.^{2}	$2\sigma_t/\bar{n}$, Å.
9	0.58×10^6	2.55×10^8	0.012×10^9	0.012×10^9	0.21	0.057
18	5.0×10^6	22×10^8	0.11×10^9	0.11×10^9	2.7	0.105
30	150×10^6	660×10^8	3.1×10^9	3.2×10^9	102	0.38
114	6800×10^6	$30{,}000 \times 10^8$	140×10^9	146×10^9	6800	0.81

static runs depicted in Figure 4 are dramatically confirmed by the sector experiments.

The mean lifetime of the radicals corresponds approximately to the reciprocal flashing frequency associated with the rise in $\bar{n}$ as the sector speed increases. In our experiments, it varies from about 0.2 to 2 sec. Diffusion to the wall occurs in comparable times. However, in some of our experiments where CO_2 was added it had no effect. Under these conditions the radical lifetime was about 0.2 sec. and the time for diffusion to the wall was many seconds. Clearly, wall reactions can play no role under these conditions. Under other conditions where diffusion to the wall could occur, no unusual results were observed. Thus, again, we can conclude that there is no evidence for any heterogeneous reaction.

We applied the theory of rotating sectors to obtain the rate constants for propagation and termination. To do so, we assumed that reaction b was instantaneous, as it surely must be considerably faster than the shortest times obtained with our sector. Also, it was necessary to assume a functional form for $k_p/k_t^{1/2}$, and we used the relationship

$$\frac{k_p}{k_t^{1/2}} = \gamma(\bar{n})^{-\delta} \qquad (7)$$

where γ and δ are constants. From Figure 4 it can be seen that such an expression is not too bad if $\bar{n}$ does not change too much. Of course, γ and δ were different for the four sets of experiments. The solutions were obtained on the IBM 7090 computer at the Aerospace Corporation, and the results are listed in Table III. At 150°, k_p increases about 23-fold and k_t about 11,700-fold as $\bar{n}$ rises from 9 to 114. If it is assumed that the activation energy for termination is zero, then A_p and A_t can be computed; their values are also listed in Table III. The collision cross sections for propagation, $\pi\sigma_p^2$, and termination, $\pi\sigma_t^2$, are evaluated. For propagation, the cross section is for only those collisions energetically capable of reacting. The values for $\pi\sigma_t^2$ were estimated for the combination of two radicals, each of length $\bar{n}/2$. Thus, these values are upper limits. If the two radicals were different, then $\pi\sigma_t^2$ would be reduced. Finally, the last column of Table III lists $2\sigma_t/\bar{n}$, which corresponds to the radical diameter of termination for two radicals, each of length $\bar{n}/2$, per monomer unit. If termination had occurred only when the reactive ends of the radicals met, then $2\sigma_t/\bar{n}$ woud have dropped as $\bar{n}$ was enhanced. In fact, $2\sigma_t/\bar{n}$ rises with $\bar{n}$, indicating that termination can occur even if the reactive sites do not join. Presumably the radicals capture each other by intertwining and then chemically react at their leisure. The corresponding increase in $\pi\sigma_p^2$ likewise suggests that a radical can trap a monomer unit before chemical reaction actually occurs.

Acknowledgment. The authors wish to thank Mr. George Takata for preparing and running the computer program, Dr. M. T. O'Shaughnessy for useful discussions, and Mrs. Barbara Peer for assistance with the manuscript. This work was supported by the U. S. Air Force under Contract No. AF 04(695)-469.